# The effect of apnea length on vital parameters in apnea of prematurity - Hybrid observations from clinical data and simulation in a mathematical model

Early Human Development 165 (2022) 105536

Contents lists available at ScienceDirect

Early Human Development

journal homepage: www.elsevier.com/locate/earlhumdev

# The effect of apnea length on vital parameters in apnea of prematurity – Hybrid observations from clinical data and simulation in a mathematical model

Gabriele Varisco [a,b,*], Irene Lensen [c], Deedee Kommers [a,d], Peter Andriessen [a,d], Peter Bovendeerd [c], Carola van Pul [a,b]

[a] Applied Physics, Eindhoven University of Technology, Eindhoven, the Netherlands
[b] Clinical Physics, Máxima Medical Center, Veldhoven, the Netherlands
[c] Biomedical Engineering, Eindhoven University of Technology, Eindhoven, the Netherlands
[d] Pediatrics, Máxima Medical Center, Veldhoven, the Netherlands

ARTICLE INFO

*Keywords:*
Prematurity
Apnea of prematurity
Oxygen desaturation
Cardio-respiratory model
Oxygen model

ABSTRACT

Apnea of prematurity (AOP) is a critical condition for preterm infants which can lead to several adverse outcomes. Despite its relevance, mechanisms underlying AOP are still unclear. In this work we aimed at improving the understanding of AOP and its physiologic responses by analyzing and comparing characteristics of real infant data and model-based simulations of AOP. We implemented an existing algorithm to extract apnea events originating from the central nervous system from a population of 26 premature infants (1248 h of data in total) and investigated oxygen saturation ($SpO_2$) and heart rate ($HR$) of the infants around these events. We then extended a previously developed cardio-vascular model to include the lung mechanics and gas exchange. After simulating the steady state of a preterm infant, which successfully replicated results described in previous literature studies, the extended model was used to simulate apneas with different lengths caused by a stop in respiratory muscles. Apneas identified by the algorithm and simulated by the model showed several similarities, including a far deeper decrease in $SpO_2$, with the minimum reached later in time, in case of longer apneas. Results also showed some differences, either due to how measures are performed in clinical practice in our neonatal intensive care unit (e.g. delayed detection of decline in $SpO_2$ after apnea onset due to signal averaging) or to the limited number of very long apneas ($\geq$80 $s$) identified in our dataset.

## 1. Introduction

Apnea of prematurity (AOP) is very common in preterm infants (gestational age <37 *weeks*) and is almost universal in low-birth weight infants below 1000 *g* [1]. It has been associated with later morbidity and other adverse outcomes [2,3]. Although definitions for apnea events vary, it is generally defined as a cessation of breathing lasting more than 20 *s*, or a cessation of breathing lasting more than 10 *s* accompanied by bradycardia (heart rate ($HR$) <100 *bpm*), desaturation (oxygen saturation ($SpO_2$) <80%) or both [1]. In some apnea events, bradycardia and desaturation occur almost immediately, while in other events these responses are delayed or even absent [4]. The length of the apnea, period in which no respiration occurs, influences the depth of the bradycardia and desaturation that are associated with the apnea. In addition, increased apnea lengths have been associated with a slower decrease in $SpO_2$, possibly due to higher initial $SpO_2$ values [5]. An initial low value of arterial $SpO_2$ is thought to cause the rapid fall in $SpO_2$ in recurrent apneas, when a second apnea follows closely on a first apnea [6]. However, in some cases a decrease in $HR$ occurs instantaneously with apnea before a fall in $SpO_2$ has occurred or even in the absence of a fall in $SpO_2$, which suggests a central mechanism for bradycardia [7].

Mechanisms underlying bradycardia during apnea are still unclear. AOP is believed to be a manifestation of physiologic immaturity of the respiratory control [2]. The respiratory center regulates a stable

*Abbreviations:* AOP, Apnea of prematurity; $HR$, Heart rate; $CI$, Chest impedance; $SpO_2$, Oxygen saturation; CASEs, Central apnea-suspected event; CASE-D, Central apnea-suspected event followed by oxygen desaturation.

* Corresponding author at: Applied Physics, Eindhoven University of Technology, Eindhoven, the Netherlands.
*E-mail address:* g.varisco@tue.nl (G. Varisco).

https://doi.org/10.1016/j.earlhumdev.2021.105536
Received 3 June 2021; Received in revised form 3 December 2021; Accepted 29 December 2021
Available online 11 January 2022

breathing pattern that adapts accurately to changes in metabolic need [8]. This center receives excitatory and inhibitory inputs from 1) higher brain centers responding to, for example, emotional or volitional stimuli, 2) mechanoreceptors in the respiratory tract avoiding overinflation of the lungs, 3) peripheral chemoreceptors in the carotid and aortic body sustaining $O_2$-, $CO_2$- and pH-levels, and 4) central chemoreceptors on the ventral medullary surface sustaining $CO_2$- and pH-levels [9]. Immaturity is thought to cause impaired breathing responses to hypercapnia and hypoxia, respectively, contributing to the occurrence and severity of AOP.

In this study, we aimed at improving the understanding of apnea and its physiologic responses in premature infants. First, we implemented an automatic detection of cessations of breathing, based on a previously published algorithm [10]. We analyzed apnea events by studying clinical patient monitoring data from preterm infants admitted to our neonatal intensive care unit. In the clinical data we investigated the effect of cessation of chest respiration motion on the $SpO_2$ and *HR* of the infant. Second, we extended a previously developed cardio-vascular model [11] with a lung mechanics model and gas exchange model in which we simulated periods of varying lengths of cessation of breathing and investigated the effect on $SpO_2$ and *HR*. We hypothesized that results from physiological data and simulations by means of mathematical modeling can enhance understanding of AOP and its etiology by confirming dependencies between presumably related variables.

## 2. Methods

### 2.1. Study population

All patients included in this study consisted of 26 very low-birth-weight infants (birth weight <1500 *g*) characterized by a gestational age <30 *weeks*. For each patient, 48 *hours* of data were extracted and used in this study. Patient demographics are presented in Table 1.

All selected patients had their *ECG*, chest impedance (*CI*) and $SpO_2$ collected using the Philips IntelliVue MX800 patients' monitors (Boeblingen, Germany), according to clinical standard. *ECG* and *CI* were measured using three *ECG* leads. Sample frequency for the *ECG* was 250 *Hz*, whereas for the *CI* was 62.5 *Hz*. $SpO_2$ was captured by PPG at 1 *Hz*. The data was stored in a data warehouse (Data warehouse connect, release B.01, Philips Medical Systems, Andover, USA) and pseudonymised before storage for further analysis.

As this study had a retrospective non-invasive nature, a waiver was provided by the medical ethical committee in accordance with the Dutch law on medical research with humans (WMO).

### 2.2. Data analysis

Patients' *ECG* and *CI* signals were processed using a central apnea detection algorithm described by Lee et al. [10]. This algorithm allows to filter out all the contributions given by cardiac artifact from the original respiration to create a filtered respiration signal. Consequently, this algorithm returns a central apnea probability function from which all events characterized by a cessation of breathing longer than 10 *s* in the *CI* can be identified as central apnea-suspected event (CASEs). The length of each CASE corresponds to that of a cessation of breathing present in the original *CI* signal. A more extensive description on the original algorithm is found in [10]. For this work, as an additional step to the Lee's algorithm, all CASEs within 10 *s* distance were combined, in line with clinical practice, where cessations of breathing close to each other are evaluated as one event knowing that the decrease in $SpO_2$ can be amplified by different consecutive apneas. All CASEs followed by a decrease in $SpO_2$ within the start of each CASE and the two minutes following its end were identified. All instances where $SpO_2 \leq 85\%$ were defined as so-called CASE-Ds (with D indicating desaturation). Definitions for desaturation differ between $SpO_2 \leq 80\%$ and $SpO_2 \leq 85\%$, but since the latter is already associated with negative outcomes [4] we recently implemented a new type of alarm for a decrease in $SpO_2$ lower than 85% as part of alarm optimization process in our neonatal intensive care unit [12]. As such we classified all instances of $SpO_2 \leq 85\%$ as desaturation.

CASEs and CASE-Ds were then divided and grouped according to the length of their cessation of breathing *L*. The following lengths *L* were considered: $10s \leq L < 20s$, $20s \leq L < 30s$, $30s \leq L < 40s$, $40s \leq L < 50s$, $50s \leq L < 60s$, $60s \leq L < 80s$, $L \geq 80s$. The subdivision was selected based on the suggestions for grouping apnea-bradycardia-desaturations proposed by Mohr et al. [5] and expanded even further to elaborate the analysis of events based on their length. As a final revision for CASEs and CASE-Ds used in our work, all CASEs that were preceded by another CASE longer than 10 *s* in the previous 120 *s* were excluded from the analysis. This characteristic was introduced to avoid the inclusion of modifications in patient signals due to the contributions of previous CASEs or CASE-Ds. Removal of CASEs and CASE-Ds preceded by CASEs shorter than 10 *s* was not considered necessary as these events do not possess the characteristics of an apnea as defined in [1]. We instead calculated the percentage of CASEs and CASE-Ds preceded in the previous 10 *s* by at least one short CASE ($L < 10s$) in order to estimate the influence of this effect. For each CASE-D, *HR* (derived from the *ECG*) and $SpO_2$ were extracted. Mean values for these two signals were then computed by considering all CASE-Ds included in each group.

**Table 1**
Characteristics for patients included in the analysis

| Count of patients | 26 |
|---|---|
| Gestational age (weeks) | 27.74 ± 0.98 |
| Postnatal days | 9.86 ± 7.40 |
| Birth weight (g) | 1039.04 ± 194.67 |
| Sex | 14 males, 12 females |
| Hours per patient considered | 48 |
| Total hours | 1248 |

### 2.3. Cardio-respiratory model

The cardio-respiratory mathematical model used in this work is an extension of previously implemented models [11]. In particular, one of these recent models was developed to simulate preterm infant physiology and consisted of a cardiovascular component with a baroreceptor model [11]. In this work we extended this model with a lung mechanics component and a gas exchange model to include the respiratory system. An overview of how these components are structured is shown in Fig. 1A.

The cardiovascular model presented in [11] is a lumped parameter model of the neonatal systemic and pulmonary circulation, adapted from Sa Couto et al. [13]. Cardiac contractile cavities and vascular compartments are described as nodes with the ability to store blood. In the contractile cavities the elastance *E* is varied during the heart cycle to simulate the contraction of the heart, causing the stored blood to flow out into systemic and pulmonary circulation. Vascular compartments are characterized by a constant compliance *C* and an unstressed volume $V_0$. These nodes are connected with segments that described flow between nodes based on pressure difference $\Delta p$ over the segment and a resistance *R* of that segment, dependent on the size of the vessel. Regulation by a baroreceptor is modeled according to Wesseling et al. [14] using the parameters provided by Ursino et al. [15,16] and was adapted for a premature infant [11]. The baroreceptor model was introduced to describe the model response to a deviation in arterial blood pressure from reference value for pressure.

A model for the lung mechanics was introduced based on the work from Albanese et al. [17], but simplified to one dead space compartment, combining the larynx, trachea and bronchi (Fig. 1B) to turn it into a 3 compartments model with lungs, dead space and chest wall. Muscle pressure is modeled as a periodically changing pressure. This generated

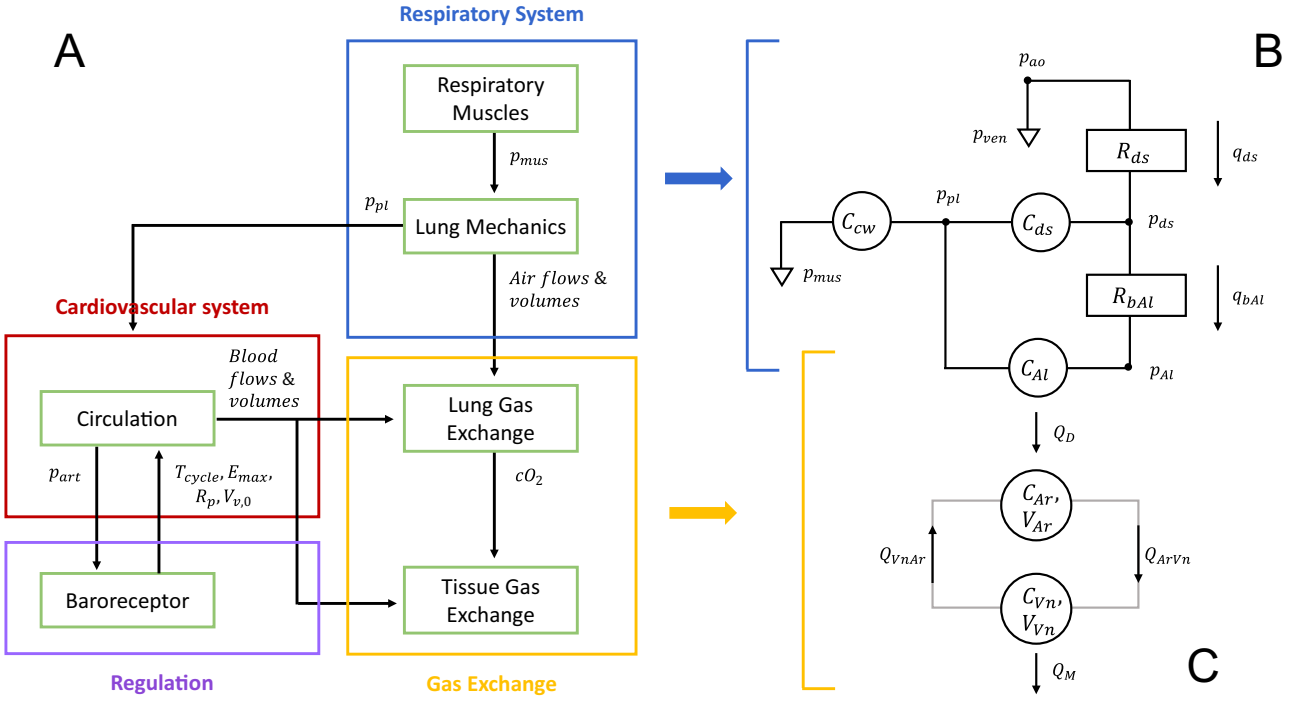


**Fig. 1.** Schematic of the cardio-respiratory model used in this work

A. Representation of the different models included in the cardio-respiratory model including their interaction. The cardiovascular system consists of the circulation which is regulated by the baroreceptor [13,14]. Blood flows and volumes, generated by the cardiovascular module, influence diffusion and metabolic rate. Diffusion rate is also dependent on oxygen flow in the lungs, caused by movement of the respiratory muscles [17]. Varying pleural pressures due to respiration affect pressures in intra-thoracic components

B. Lung mechanics model: simplified from Albanese et al. [17] into one compartment. Pressures $p$ are indicated at the nodes. Segments represent resistances $R$ and nodes compliances $C$. Flows over the resistances are visualized with arrows

C. Gas exchange model: subscripts: *ao* – airway opening, *ds* – dead space, *bAl* – bronchi to alveoli, *Al* – alveoli, *pl* – pleura, *cw* – chest wall, *mus* – respiratory muscles, *ven* – ventilator. Abbreviations: $cO_2$ – oxygen concentration, $E_{max}$ - maximum elastance, $p_{art}$ - arterial pressure, $p_{mus}$ - muscle pressure, $p_{pl}$ – pleural pressure, $R_p$ - peripheral resistance, $T_{cycle}$ - cardiac cycle time, $V_{v,\,0}$ - unstressed venous volume.

pressure changes inside the lungs, driving the air flows in and out, thus creating changes in the volumes. A more in-depth description of this model is presented in Appendix A.

Gas exchange was modeled within the lung compartment as one alveolus (Fig. 1C). The amount of oxygen stored in a node is determined by oxygen concentration in the blood bound to hemoglobin and the difference in oxygen pressure between alveoli and pulmonary micro-circulation. Oxygen saturation $SpO_2$ is then calculated from the partial oxygen pressure $pO_2$ according to the Hill equation [18]. Further details about this model are presented in Appendix B. The amount of oxygen $V_{O_2}$ in a node changed due to convective transport $Q_c$, diffusive transport $Q_D$, and metabolic rate $Q_M$ in the systemic arterial micro-circulation. Oxygen uptake occurred in the pulmonary micro-circulation and depended on capillary gas exchange parameters.

### 2.4. Model simulations

An Euler forward integration scheme was used to solve the model numerically. The model was solved for every time step $\Delta t$. Changes in air and blood volume, pressure and flow were calculated by taking the volume at the current time point $t_n$ as a starting point.

All cardiovascular and baroreceptor parameters were estimated to simulate a one week old preterm infant with a gestational age of 28 *weeks* and birth weight of 1000 *g*, using scaled parameters according to Jennekens et al. [11], who scaled values for a full term infant from Sa Couto et al. [13]. Lung mechanics parameters were used from Albanese et al. [17] and scaled down similarly to Jennekens' method [11]. Parameters for the oxygen model were based on literature [13,17–20]. The cardiac output was estimated as 175 *ml/min* and the total blood volume of the infant at 110 *ml* [11]. Parameters for both the lung mechanics and gas exchange models are shown in Appendix C.

Before simulating apnea with our model, we investigated whether the steady state of the model simulated a preterm infant adequately. Therefore, we modeled a preterm infant until steady state had been reached. Hemodynamic outputs of the model were compared with reference values provided in [21,22]. Particular attention was also dedicated to the parameters for the respiratory model as well as the oxygen levels as these are especially relevant for the modeling of apnea: these parameters were compared with the reference values from [23–25].

Apnea was simulated by adjusting lung mechanics parameters to simulate a cessation of breathing caused by a stop in respiratory muscles (i.e. respiration rate, $RR = 0$), similarly to what happens in premature infants for apneas with a central origin. The model was run for multiple apnea lengths to study the effect of apnea length on vital signs, and the outcomes of the model were studied and compared with CASE-Ds from real infants data. Cessations of breathing with different lengths $L$ were included in this work to mimic the apnea periods from the data study. We therefore choose to model apnea lengths of 10, 20, 30, 40, 50, 60 and 80 *s*.

Apnea was also simulated after varying the value of different parameters: these included the initial respiration rate ($RR$), metabolic rate ($Q_M$) and alveolar compliance ($C_{Al}$). In literature, an increase in oxygen levels preceding very long apneas caused by an increase in $RR$ was described by Mohr et al. [5]. They hypothesized that this increase in $SpO_2$ caused a decrease in the slope of $SpO_2$. To verify this finding in our model we simulated increased $SpO_2$ values before apnea by increasing the $RR$ at start in our model. Reference $RR$, set equal to 49 *bpm*, was

multiplied by factors 0.9, 1, 1.1 and 1.2. These factors were estimated so that $SpO_2$ values laid in the range reported in [5], as no average *RR* were reported. Outcomes obtained with different *RR* were then studied and compared with each other. Initial $Q_M$ was set equal to 0.12 $ml O_2/s$, as estimated by previous works considering a population of preterm infants [26,27]. Different apneas were then generated using the model by multiplying this value by factors 0.5, 0.8, 1 and 1.2, selected to consider a wide number of possibilities for this parameter. Different $C_{Al}$ were evaluated due to the influence of alveolar stiffness on the tidal volume of the premature infants, a characteristic which could significantly affect the simulated apneas. $C_{Al}$ was initially set equal to 0.93 $ml/cmH_2O$ following [17] and multiplied by factors 0.5, 0.8, 1 and 1.5 to estimate its contribution on the simulated apneas.

## 3. Results

The total count of CASEs and CASE-Ds is presented in Table 2. The count of events for each group decreased when longer lengths *L* were considered. This table also reports the mean count and standard deviation of CASE-Ds computed per patient as well as the mean ratio between the count of CASE-Ds and CASEs. 64.5% of CASEs and 59.7% of CASE-Ds included in this work were preceded by at least one short CASE in the 10 *s* preceding their onset.

A mean representation of *HR* and $SpO_2$ for CASE-Ds considering the different *L* is presented in Fig. 2. All mean curves for both *HR* and $SpO_2$ for CASE-Ds with $L < 80s$ (Fig. 2A–B) shared the property that their minimum value is reached later in time when longer CASE-Ds are considered. For each length *L*, the minimum *HR* value was always occurring earlier in time compared to the minimum $SpO_2$ value. CASE-Ds with $L \geq 80s$ showed different patterns from what was shown by shorter CASE-Ds. Curves for mean *HR* and $SpO_2$ for CASE-Ds with $L \geq 80s$ (Fig. 2C–D) presented several oscillations which were not present in shorter CASE-Ds, possibly indicating the contribution of multiple shorter CASEs. An additional analysis computed separately for each CASE-Ds with $L \geq 80s$ showed brief moments of recovery from cessations of breathing for different patients. These interruptions between long periods without breathing-related motion in the CI signal explain why there are some prominent peaks and troughs in the mean curves.

The cardio-respiratory and oxygen models were used to simulate a stable preterm infant, for which results are presented in Fig. 3. The outcomes of this new combined model showed that the oxygen pressures in the arteries and veins remained constant at approximately 60 and 32 *mmHg*, respectively (Fig. 3A). $SpO_2$ levels in lung microcirculation and pulmonary vein reached 95%, since parameters were adjusted to match this value (Fig. 3B). The volume of the alveoli fluctuated with a tidal volume of 2.3 *ml*, while dead space remained mostly constant (Fig. 3C).

Apnea was simulated by generating cessation of respiration motion at $t = 0$ *s*. Results for these experiments, obtained with different apnea lengths are presented in Fig. 4A. During apnea, arterial $SpO_2$ decreased, with a total decrease in $SpO_2$ of 5%, 12%, 17%, 22%, 27%, 32% and 43% for apnea lengths *L* of 10, 20, 30, 40, 50, 60 and 80 *s*, respectively. During apnea, the slope of $SpO_2$ was independent of length *L*. However, the rate of recovery of the arterial $SpO_2$ increased with increasing *L*. Simulations while varying the *RR*, $Q_M$ and $C_{Al}$ are shown in Fig. 4B–D. Higher respiration rate (*RR*) caused an increase in the initial $SpO_2$, which was respectively found to be equal to 92%, 94%, 95% and 96%, as shown in Fig. 4A. Higher initial *RR* resulted in a slower decrease in the initial phase after the apnea and to a higher rate of recovery of the arterial $SpO_2$. Higher metabolic rate ($Q_M$) resulted in a progressively steeper decrease in $SpO_2$ and led to progressively lower minimum values which were equal to 89%, 74%, 63% and 51%, respectively. $SpO_2$ recovery was also affected by this parameter. The effect of different $C_{Al}$ on the generated apneas was very limited: higher $C_{Al}$ mildly affected the initial $SpO_2$ but had no influence neither on $SpO_2$ decay nor on its recovery after the minimum was reached.

All apnea simulations also presented a common pattern for the *HR*: after a slight decrease that follows the start of the apnea, *HR* increased from 142.2 to 143.0 *bpm* irrespectively of the apnea lengths. When apnea ended, *HR* decreased to its original value of 142.2 *bpm*. This effect is due to the baroreceptor but is not shown by our results obtained with clinical data.

## 4. Discussion

The analysis performed with our population of preterm infants showed interesting similarities with the work from Mohr et al. [5].

A first result shared by both works indicates that the observed decline in *HR* starts most commonly before the decline in $SpO_2$ [5]. This result is also in accordance with other previous works including the one from Carbone et al. in which it is mentioned that a drop in *HR* preceded the one in $SpO_2$ in 57% of long apnea ($L \geq 20$ *s*), in 56% of medium apnea ($15 - 19$ *s*), and in 41% of short apnea ($10 - 14$ *s*) [4]. Joshi et al. in a study related to time-relationship among cessation of breathing, bradycardia and desaturation alarms also reported that bradycardia has a much higher likelihood of being followed by desaturation (37% vs. 11.5%) than vice versa and indicated a much shorter median time for the transition from one event to the other (0.7 *min* vs. 18 *min*) [28]. However, it is difficult to draw any conclusion from these observations because of two time-delays in the measurement of $SpO_2$. The measuring device has an averaging time set in our practice to 10 *s* and there is a circulation delay between blood in the lungs and blood measured in the hand or foot, which may be around $6 - 8$ *s* in our infants. This information can be estimated considering that the blood volume in premature infants is around $65 - 80$ *mL/Kg* [29,30] and the cardiac output is around 0.23 *l/min* [31], corresponding to a total circulation time (blood volume/cardiac output) of around 20 *s*. Since the blood volume in veins is about twice the amount present in arteries, the circulation delay can be estimated in the vicinity of 7 *s*. Thus, the total delay in the two measurements may be around $17 \pm 2$ *s*. This is consistent with the observations presented in Fig. 2, which show $SpO_2$ beginning to fall around 17 *s* after the cessation of breathing. It follows that we cannot conclude just from these observations whether the drop in *HR* actually begins before or after the drop in $SpO_2$.

Differently from what is described in [5], we observed the decline in *HR* starting slightly before the cessation of breathing. We do not expect this to be a result of timing errors in the monitoring system. We found however that 59.7% of CASE-Ds were preceded by short CASEs in the previous 10 *s* (indicating the presence of cessations of breathing shorter than 10 *s*). We acknowledge that short cessations of breathing preceding the actual CASE-Ds could have contributed to a drop in *HR* in multiple

**Table 2**
Count of central apnea-suspected events (CASEs) and central apnea suspected events followed by a decrease in oxygen saturation ($SpO_2$) ≤ 85% (CASE-Ds), median and percentiles [25,75] of CASE-Ds and median ratio CASE-Ds/CASEs computed per patient. All values are presented for different lengths for the cessations of breathing L

| Measure | 10s ≤ L < 20s | 20s ≤ L < 30s | 30s ≤ L < 40s | 40s ≤ L < 50s | 50s ≤ L < 60s | 60s ≤ L < 80s | L ≥ 80s | ALL |
|---|---|---|---|---|---|---|---|---|
| # CASEs | 3140 | 655 | 404 | 202 | 106 | 127 | 122 | 4756 |
| # CASE-Ds ($SpO_2 \leq 85$) | 646 | 190 | 120 | 60 | 31 | 43 | 28 | 1118 |
| Median CASE-Ds | 13.5 | 5.5 | 2.5 | 1 | 0 | 1 | 1 | 25.5 |
| Percentiles [25,75] CASE-Ds | [3,43] | [1,11] | [1,7] | [0,3] | [0,2] | [0,3] | [0,1] | [10, 74] |
| Median ratio CASE-Ds/ CASEs | 0.13 | 0.26 | 0.25 | 0.20 | 0.24 | 0.47 | 0.20 | 0.17 |

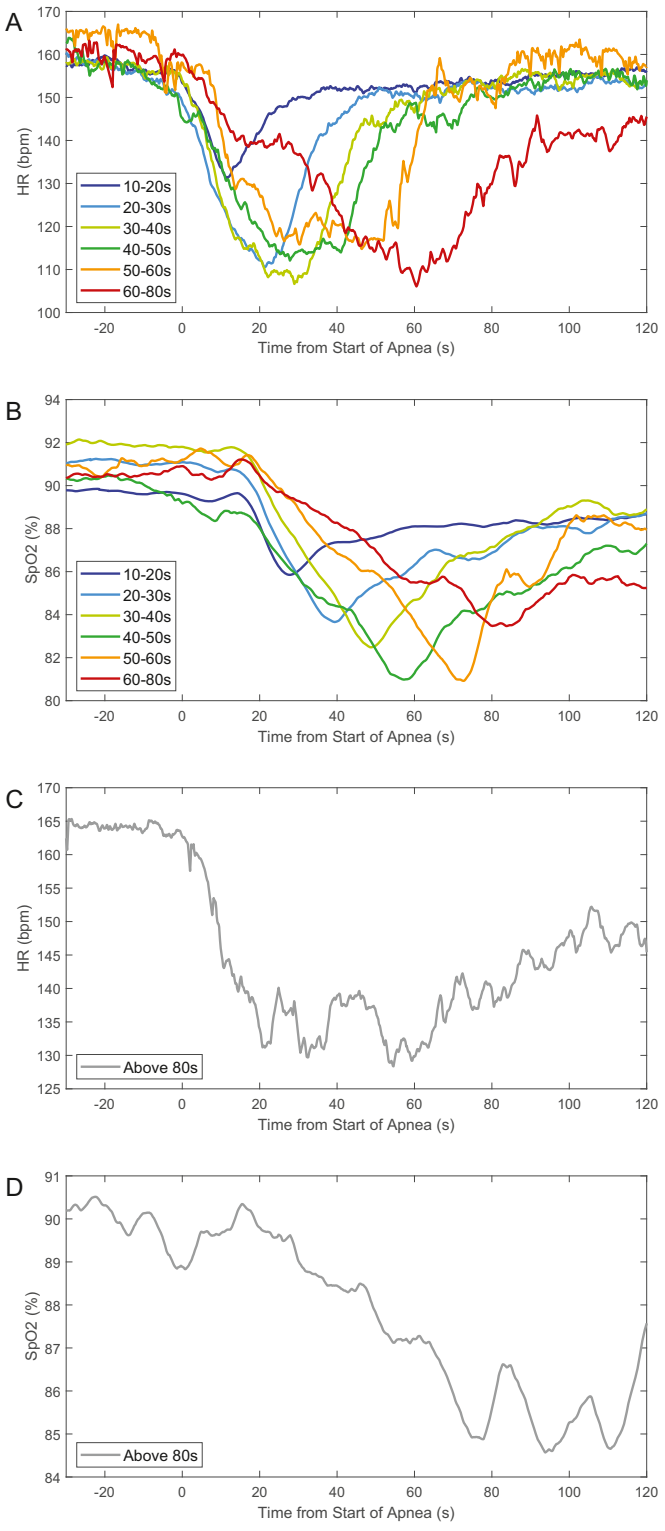


**Fig. 2.** Mean representation of heart rate (*HR*) and oxygen saturation ($SpO_2$) curves for central apnea-suspected events followed by a decrease in $SpO_2 \leq 85$ % (CASE-Ds) considering the different lengths of the cessation of breathing *L*. *HR* and $SpO_2$ curves for CASE-Ds with $10s \leq L < 20s$, $20s \leq L < 30s$, $30s \leq L < 40s$, $40s \leq L < 50s$, $50s \leq L < 60s$, $60s \leq L < 80s$ are presented in (**A**) and (**B**). *HR* and $SpO_2$ curves for CASE-Ds with $L \geq 80$ *s* are presented in (**C**) and (**D**). All patients included in the dataset are included in these representations.

occasions but nonetheless we did not consider the exclusion of CASE-Ds preceded by short CASEs from our study since these short CASEs do not comply with the definition of apnea presented in [1]. The drop in *HR* happening before the cessation of breathing indicates that this drop in HR could not be caused by the drop in $SpO_2$ since the decrease in saturation is a direct consequence of the interruption in the breathing motion. The drop in *HR* preceding the cessation of breathing suggests therefore that other mechanisms may be involved, such as a central mechanism for bradycardia, or a central mechanism producing both bradycardia and apnea. However, the presence of short CASEs prior to the long apneas studied in this work makes it difficult to draw any definitive conclusion.

Other important similarities with the work of Mohr et al. included minimum $SpO_2$ values appearing later in time and lower values in case of longer cessations of breathing, for all $L < 80$ *s*. In addition, longer decreases in *HR* were also found in case of longer cessations of breathing. Mohr et al. suggested that the slower decrease in $SpO_2$ for longer cessations of breathing could be related to the elevated $SpO_2$ values that they found before very long apneas, a characteristic which was possibly caused by an increase in *RR* [5]. This hypothesis was supported by a model analysis of arterial oxygen desaturation during apnea in a preterm infant by Sands et al. [6]. However, we cannot confirm elevated $SpO_2$ values before the start of longer cessations of breathing in our dataset.

By looking at apneas extracted from our population of premature infants we also noticed that the rate of decrease in $SpO_2$ seemed to slow down as the length of the cessation of breathing increased. We hypothesize that the respiratory centers might be triggered by the rate of decrease in $SpO_2$, leading to a faster trigger of the respiratory muscles in case of higher rates of decrease, typical of shorter apneas, and thus stopping apnea with a quicker response. Recovery of $SpO_2$values found before the start of the cessation of breathing was also found to happen earlier in time in case of shorter CASE-Ds, similarly to what is presented in [5].

In our study, *HR* and $SpO_2$ curves for CASE-Ds longer than 80 *s* showed different patterns compared to the curves from shorter CASE-Ds. We observed for $L \geq 80$ *s* a smaller decrease in $SpO_2$ than for shorter cessations of breathing. This result can be explained by the fact that these CASE-Ds were often the result of the combination of short CASEs and in the time frame between each CASE the patient had possibly taken a breath to adjust $SpO_2$ levels. This result was verified with a separate analysis of each CASE-Ds longer than 80 *s*, which indicated an overlap for the most prominent peaks and troughs in the *HR* and $SpO_2$ in both single CASE-Ds and in the mean curves included in Fig. 2C–D. Furthermore, these modification in *HR* and $SpO_2$ resulted being associated to brief interruptions in the cessations of breathing, proving that CASE-Ds longer than 80 *s* often resulted from the combination of short CASEs. Note that this combination did not frequently occur in the other CASE-D groups, as mean representations included in Fig. 2A–B did not include the same fluctuations in *HR* and $SpO_2$ as shown in Fig. 2C–D.

Our simulations in the stable premature cardiovascular system showed that, with the addition of the respiratory models, our model was able to simulate the physiology of a premature infant as values calculated in our model are in line with reference values from literature for both cardiovascular parameters [21,22,32,33] and for oxygen and partial oxygen pressures [23–25]. An exception, however, is the venous $SpO_2$ level, as in our model this showed higher values than those found in literature [23]. This might be attributed either to the fact that the values found in literature refer to preterm infants with different postnatal ages or to the choices made in the model with respect to parameters, as not all parameters can be easily measured and they are estimated based on literature studies.

In response to the different simulated apneas, the total decrease in $SpO_2$ was smaller in shorter apneas, as breathing resumed earlier. Recovery of the initial $SpO_2$ values was also found to happen faster in case of shorter apneas. This result reflects the findings in the data from our population of preterm infants for CASE-Ds shorter than 80 *s*, and they

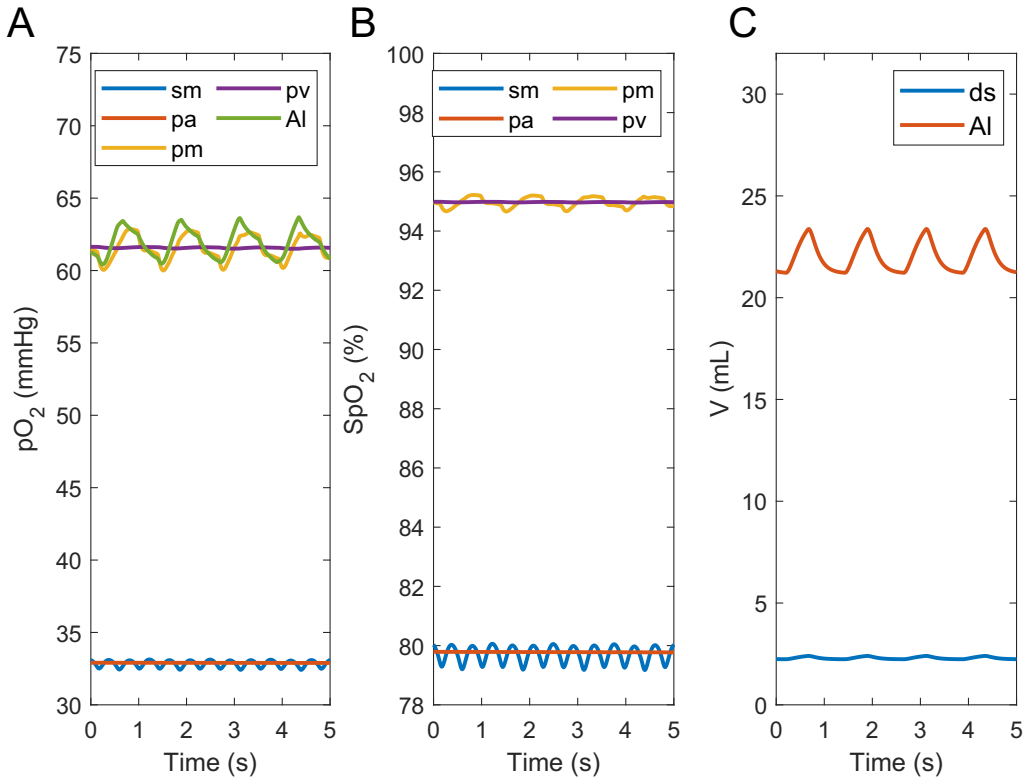


**Fig. 3.** (**A**) Simulated oxygen partial pressure ($pO_2$), (**B**) oxygen saturation ($SpO_2$) and lung volume $V$ (**C**) as a function of time for a preterm infant according to original model under baroreceptor control. Abbreviations: *Al* - alveolar, *ds* - dead space, *pa* - pulmonary artery, *pm* - pulmonary micro-circulation, *pv* - pulmonary vein, *sm* - systemic micro-circulation.

are in line with values found in literature [4,34].

During apnea simulation, arterial $SpO_2$ showed a biphasic response in our model, a result not easily recognizable in our data. Results from the model showed that initially $SpO_2$ decreased rapidly. This steep decrease was then followed by a slower decrease. This biphasic response to apnea is not widely discussed in literature, however, it was observed in some studies [35,36]. Later, this phenomenon was investigated and confirmed in other studies [6,37]. In the model, systemic arterial oxygen pressure closely followed alveolar oxygen pressure. Under normal conditions, systemic venous oxygen pressure was about 30 *mmHg* lower. During early apnea, this difference in oxygen pressure led to a large diffusive rate that quickly drained oxygen from the alveoli causing both alveolar and arterial pressure to drop. When alveolar and arterial oxygen pressure approached venous oxygen pressure, essentially alveoli and the blood could be considered to behave as one single oxygen storage compartment, from which oxygen was consumed at a constant metabolic rate. This caused the constant rate of decrease in $SpO_2$ in our model, whereas in the data we observed that the decrease depends on the apnea length. This constant slope in the model is explained by the choice that metabolic consumption was assumed independent of apnea length. This result was found since the threshold $CO_{2,\,th}$ was not reached during our simulations. In case this threshold was overcome oxygen consumption would have dropped, directly affecting the slope of decrease as shown for apneas extracted from our patients.

The influence of the setting of other parameters, namely $RR$, $Q_M$ and $C_{Al}$, on the simulated apneas was investigated. $RR$ determined the steady state level of arterial $SpO_2$ and affected the rate at which this level dropped during early apnea. $Q_M$ directly determined the rate of decrease in $SpO_2$ during late apnea. $C_{Al}$, an important parameter since low values are associated with a higher risk of respiratory distress syndrome, showed very limited contributions on the simulated apneas. Since the estimation of $Q_M$ (both value and its independence on apnea length) largely influences the extent of the decrease in $SpO_2$, improving the estimation based on clinical data could improve apnea simulation.

Following a simulated apnea, the model showed a slight raise in $HR$, caused by the response to the baroreflex regulation. Our model was not able to simulate the observed drop in $HR$ following CASE-Ds in our data. The modeled increase in $HR$ was due to the increase of the intrathoracic pressure during apnea, resulting in a decrease in cardiac filling. Following the Starling effect [38] this led to a decrease in cardiac output and arterial pressure. However, this rise in $HR$ was very small ($<0.8$ *bpm*), and thus physiologically irrelevant. To explain the large decrease in $HR$ found in our experimental data, our model should be extended with additional regulatory mechanisms, responding to inputs from the chemoreceptors and the lung stretch receptors. Notably, some studies claimed that the fall in $HR$ is a chemoresponse to the fall in $SpO_2$ resulting from apnea, because of the significant correlation between the decrease in $SpO_2$ and $HR$ [39]. However, our data suggests that the fall in $HR$ precedes the fall in $SpO_2$, making this mechanism less plausible.

Results provided in this work allowed to compare CASE-Ds extracted from physiological data of premature infants with simulations of apnea from a cardio-respiratory model. These results shared different similarities including a far deeper decrease in $SpO_2$, where the minimum was reached later in time, in case of longer apneas. Furthermore, in both CASE-Ds and apnea simulations the initial $SpO_2$ levels are reached earlier after the minimum has been reached in case these events are shorter events. Some differences between the results could be explained either looking at how measures are performed in clinical practice in our neonatal intensive care unit (e.g. delayed decline in $SpO_2$ after apnea onset) and considering the limited number of recorded CASE-Ds within a certain group (e.g. CASE-Ds longer than 80 *s*) and the presence of short CASEs which often preceded CASE-Ds extracted from our dataset of premature infants. In addition to these, the slope of decrease in $SpO_2$ during simulated apneas was found to be the same for each apnea length since the simulated conditions of the infant before each apnea were the same for every situation, a condition that is not found in real patients.

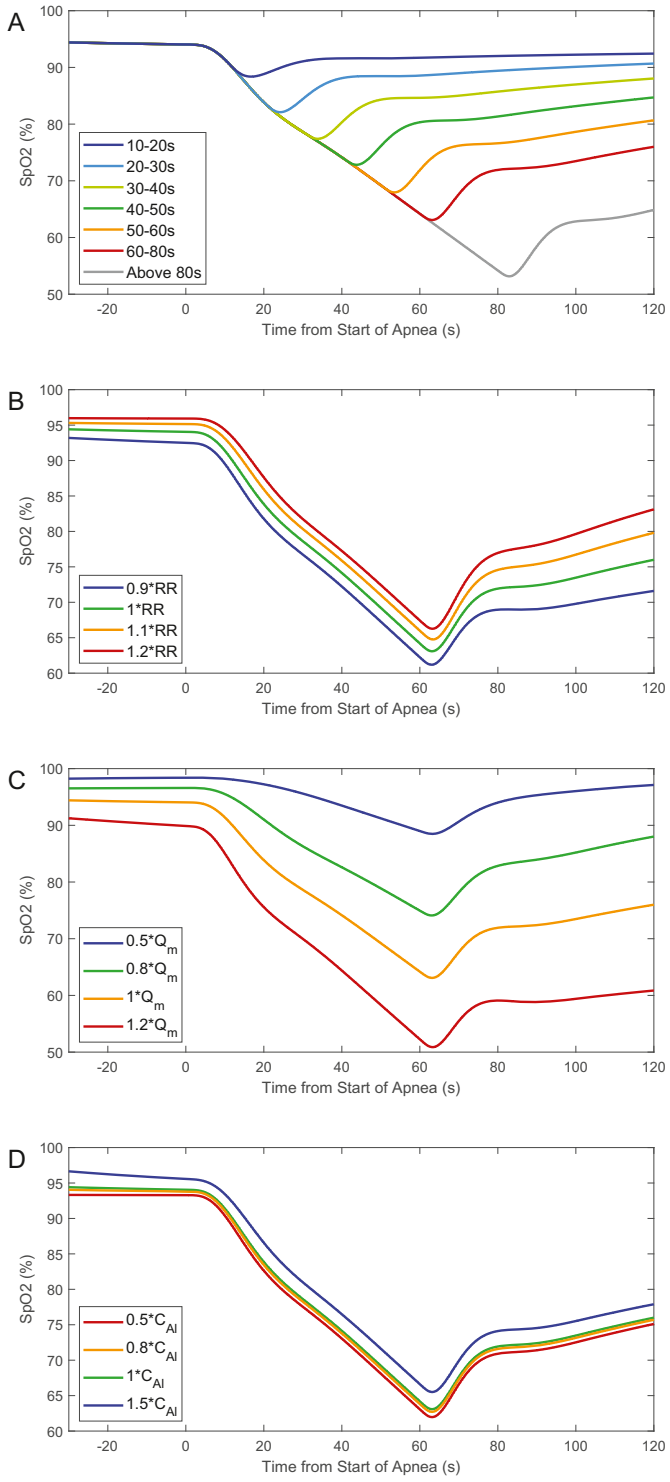


**Fig. 4.** Oxygen saturation ($SpO_2$) curves obtained by simulating apneas with different lengths of the cessation of breathing $L$ (**A**) and by varying the initial respiration rate ($RR$) (**B**), metabolic rate ($Q_M$) (**C**) and alveolar compliance ($C_{Al}$) (**D**). Variations of the different parameters that were evaluated are reported in each figure. In all figures apnea starts at $t = 0s$ by setting $RR = 0$. Reference RR is equal to 49 *bpm*, reference $Q_M$ is equal to 0.12 $mlO_2/s$ and compliance $C_{Al}$ is equal to 0.93 $ml/cmH_2O$.

Finally, an important limitation is the missing contribution of chemoreceptors and lung stretch receptors, that might affect the metabolic rate $Q_M$, which was assumed to remain constant during apnea during our simulations. Future studies should also try to model the fall in *HR* and possibly get us a better understand of the underlying mechanisms that cause this fall, taking into account the contribution from the chemoreceptor, similarly to what was described by Albanese et al. [17]. Another limitation of our model is that it only allows to simulate central apneas while at the moment other types of apneas cannot be simulated. Nevertheless, our cardio-respiratory model was successfully able to replicate the steady state of premature infants and describe the decay in $SpO_2$ during apnea, showing results in line with different literature studies.

## 5. Conclusion

The aim of this study was to combine the use of modeling data and real infant data to enhance understanding of AOP and as such, confirm dependencies between variables known to influence AOP. By analyzing CASE-Ds in real infant data, we showed that longer cessations of breathing were followed by a slower decrease in *HR* and $SpO_2$. The decrease in *HR* was also found to occur before the decrease in $SpO_2$. By extending an existing cardiovascular model to include a lung mechanics and a gas exchange compartment and by fitting parameters for a preterm infant, we were able to simulate different characteristics found in CASE-Ds, i.e. the drop in $SpO_2$ during apneas as well as a deeper decline in $SpO_2$ for longer apneas. Our model did not allow yet to simulate the decrease in *HR*, an observation which might be reproduced by introducing the chemoreceptors and lung stretch receptors in the model.

## Declaration of competing interest

The authors declare no conflict of interest

## Acknowledgment

This work was done within the framework of the Eindhoven MedTech Innovation Center (e/MTIC) which is a collaboration of the Eindhoven University of Technology, Philips Research, and MMC. This work is a result of the ALARM project funded by the Nederlandse Organisatie voor Wetenschappelijk Onderzoek (NWO) grant number 15345.

## Appendix A. Supplementary data

Supplementary data to this article can be found online at https://doi.org/10.1016/j.earlhumdev.2021.105536.

## References

[1] N.N. Finer, R. Higgins, J. Kattwinkel, R.J. Martin, Summary proceedings from the apnea-of-prematurity group, Pediatrics 117 (3) (2006) S47–S51.
[2] J.M. Abu-Shaweesh, R.J. Martin, Neonatal apnea: what's new? Pediatr. Pulmonol. 43 (10) (2008) 937–944.
[3] C.F. Poets, et al., Association between intermittent hypoxemia or bradycardia and late death or disability in extremely preterm infants, JAMA, J. Am. Med. Assoc. 314 (6) (2015) 595–603.
[4] T. Carbone, L.C. Marrero, J. Weiss, M. Hiatt, T. Hegyi, Heart rate and oxygen saturation correlates of infant apnea, J. Perinatol. 19 (1) (1999) 44–47.
[5] M.A. Mohr, et al., Very long apnea events in preterm infants, J. Appl. Physiol. 118 (5) (2015) 558–568.
[6] S.A. Sands, B.A. Edwards, V.J. Kelly, M.R. Davidson, M.H. Wilkinson, P.J. Berger, A model investigation of the impact of ventilation-perfusion mismatch on oxygenation during apnea in preterm infants, J. Theor. Biol. 264 (3) (2010) 657–662.
[7] O.P. Mathew, Apnea of prematurity: pathogenesis and management strategies, J. Perinatol. 31 (5) (2011) 302–310.
[8] J.M. Di Fiore, R.J. Martin, E.B. Gauda, Apnea of prematurity - perfect storm, Respir. Physiol. Neurobiol. 189 (2) (2013) 213–222.
[9] J.L. Feldman, C.A. Del Negro, P.A. Gray, Understanding the rhythm of breathing: so near, yet so far, Annu. Rev. Physiol. 75 (2013) 423–452.
[10] H. Lee, et al., A new algorithm for detecting central apnea in neonates, Physiol. Meas. 33 (1) (2012) 1–17.
[11] W. Jennekens, M. Dat, P.H.M. Bovendeerd, P.F.F. Wijn, P. Andriessen, Validation of a preterm infant cardiovascular system model under baroreflex control with heart rate and blood pressure data, Proc. Annu. Int. Conf. IEEE Eng. Med. Biol. Soc. EMBS (2011) 896–899.

[12] G. Varisco, et al., Optimisation of clinical workflow and monitor settings safely reduces alarms in the NICU, Acta Paediatr. Int. J. Paediatr. 110 (4) (2021) 1141–1150.
[13] C.D. Sá Couto, W.L. Van Meurs, J.A. Goodwin, P. Andriessen, A model for educational simulation of neonatal cardiovascular pathophysiology, Simul. Healthc. (1) (2006) 4–12.
[14] J. Wesseling, K. Settels, Circulatory model of baro-and cardio-pulmonary reflexes, IOS Press, 1993, pp. 56–67.
[15] M. Ursino, Interaction between carotid baroregulation and the pulsating heart: a mathematical model, Am. J. Physiol. Hear. Circ. Physiol. 275 (5) (1998) 1733–1747, 44-5.
[16] M. Ursino, E. Magosso, Role of short-term cardiovascular regulation in heart period variability: a modeling study, Am. J. Physiol. Hear. Circ. Physiol. 284 (4) (2003) 1479–1493, 53-4.
[17] A. Albanese, L. Cheng, M. Ursino, N.W. Chbat, An integrated mathematical model of the human cardiopulmonary system: model development, Am. J. Physiol. Hear. Circ. Physiol. 310 (7) (2016) H899–H921.
[18] W.E.L. Brown, A.V. Hill, in: The Oxygen-Dissociation Curve of Blood 94, Royal Society, 1922, pp. 297–334 (661).
[19] M. Delivoria-Papadopoulos, N.P. Roncevic, F.A. Oski, Postnatal changes in oxygen transport of term, premature, and sick infants: the role of red cell 2,3-diphosphoglycerate and adult hemoglobin, Pediatr. Res. 5 (6) (1971) 235–245.
[20] K. Bauer, C. Uhrig, P. Sperling, K. Pasel, C. Wieland, H.T. Versmold, Body temperatures and oxygen consumption during skin-to-skin (kangaroo) care in stable preterm infants weighing less than 1500 grams, J. Pediatr. 130 (2) (1997) 240–244.
[21] R.M. Kliegman, B. Stanton, J.S. Geme, N. Schor, R.E. Behrman, Nelson Textbook of Pediatrics, Elsevier, 2011.
[22] K. Charles, S. Istvan, Hemodynamics and Cardiology: Neonatology Questions and Controversies, 2012.
[23] A. Castillo, et al., Pulse oxygen saturation levels and arterial oxygen tension values in newborns receiving oxygen therapy in the neonatal intensive care unit: is 85% to 93% an acceptable range? Pediatrics 121 (5) (2008) 882–889.
[24] S.P. Wardle, A.M. Weindling, Peripheral oxygenation and anemia in preterm babies, Pediatr. Res. 44 (1) (1998) 125–131.
[25] P. Latzin, et al., Lung volume, breathing pattern and ventilation inhomogeneity in preterm and term infants, PLoS One 4 (2) (2009).
[26] H. Suga, Total mechanical energy of a ventricle model and cardiac oxygen consumption, Am. J. Physiol. 236 (3) (1979).
[27] H. Suga, R. Hisano, S. Hirata, Heart rate-independent energetics and systolic pressure-volume area in dog heart, Am. J. Physiol. - Hear. Circ. Physiol. 13 (2) (1983).
[28] R. Joshi, C. Van Pul, L. Atallah, L. Feijs, S. Van Huffel, P. Andriessen, Pattern discovery in critical alarms originating from neonates under intensive care, Physiol. Meas. 37 (4) (2016) 564–579.
[29] K. Bauer, O. Linderkamp, H.T. Versmold, Systolic blood pressure and blood volume in preterm infants, Arch. Dis. Child. 69 (1993) 521–522.
[30] N. Aladangady, S. McHugh, T.C. Aitchison, C.A.J. Wardrop, B.M. Holland, Infants' blood volume in a controlled trial of placental transfusion at preterm delivery, Pediatrics 117 (1) (2006) 93–98.
[31] K.H. Hsu, T.W. Wu, Y.C. Wang, W.H. Lim, C.C. Lee, R. Lien, Hemodynamic reference for neonates of different age and weight: a pilot study with electrical cardiometry, J. Perinatol. 36 (6) (2016) 481–485.
[32] A.L. Kent, S. Meskell, M.C. Falk, B. Shadbolt, Normative blood pressure data in non-ventilated premature neonates from 28–36 weeks gestation, Pediatr. Nephrol. 24 (1) (2009) 141–146.
[33] V. Soloveychik, A. Bin-Nun, A. Ionchev, S. Sriram, W. Meadow, Acute hemodynamic effects of caffeine administration in premature infants, J. Perinatol. 29 (3) (2009) 205–208.
[34] N.N. Finer, K.J. Barrington, B.J. Hayes, A. Hugh, Obstructive, mixed, and central apnea in the neonate: physiologic correlates, J. Pediatr. 121 (6) (1992) 943–950.
[35] E.C. Fletcher, R. Kass, J.I. Thornby, J. Rosborough, T. Miller, Central venous O2 saturation and rate of arterial desaturation during obstructive apnea, J. Appl. Physiol. 66 (3) (1989) 1477–1485.
[36] N. Iwase, et al., Effects of repetitive airway obstruction on O2 saturation and systemic and pulmonary arterial pressure in anesthetized dogs, Am. Rev. Respir. Dis. 146 (6) (1992) 1402–1410.
[37] M.H. Wilkinson, P.J. Berger, N. Blanch, V. Brodecky, Effect of venous oxygenation on arterial desaturation rate during repetitive apneas in lambs, Respir. Physiol. 101 (3) (1995) 321–331.
[38] A.M. Katz, Ernest Henry Starling, his predecessors, and the 'Law of the heart', Circulation 106 (23) (2002) 2986–2992.
[39] D.J. Henderson-Smart, M.C. Butcher-Puech, D.A. Edwards, Incidence and mechanism of bradycardia during apnoea in preterm infants, Arch. Dis. Child. 61 (3) (1986) 227–232.